JOURNAL OF MATERIALS SCIENCE **40** (2005) 1393– 1398

Monte Carlo modelling of hole transport in MDMO-PPV: PCBM blends

A. J. CHATTEN*, S. M. TULADHAR, S. A. CHOULIS, D. D. C. BRADLEY, J. NELSON
Physics Department, Imperial College, London, SW7 2BW, UK

We propose a model of hole transport in interpenetrating two-phase systems and apply it to blends of poly[2-methoxy-5-3(3′,7′-dimethyloctyloxy)-1-4-phenylene vinylene], (MDMO-PPV), and 1-(3-methoxycarbonyl)-propyl-1-phenyl-(6,6)C_{61}, (PCBM) with low PCBM content. The main features of the model are that hole transport is mediated by a small polaron tunnelling expression and that the density of states contains a tail of deep traps, which serve to delay carrier transport. The exponential factor governing the depth of these localised states is derived from transient optical measurements. The model is implemented using Monte Carlo simulations and is applied to reproduce both the time of flight hole photocurrent transients and the field dependence of the hole mobilities extracted from the data. We show that the transport behaviour detected by time of flight and transient absorption spectroscopy can be described quantitatively with a single transport model.

1. Introduction

The optical and electronic properties of semiconducting polymer films have recently been extensively studied for applications in light emitting diodes, field effect transistors and solar cells [1, 2]. Early photovoltaic devices, fabricated from donor/acceptor bilayers yielded low power conversion efficiencies since the exciton diffusion length (typically 10 nm) is significantly less than the thickness required for efficient light absorption. A breakthrough in increasing the efficiency was achieved by the introduction of the bulk heterojunction. Intimate blending of materials of suitable electron affinities and ionisation potentials leads to a three-dimensional heterojunction on the 10 nanometer scale [3, 4]. This phase separation on the mesoscale ensures efficient charge separation because excitons are always generated within an exciton diffusion length of the interface, and are likely to dissociate into charge pairs. The blend also provides continuous pathways in each material for charge conduction to the external electrodes provided that the volume fraction of each component is sufficient for percolation.

Blends of a hole transporting conjugated polymer with an electron accepting fullerene derivative are particularly promising for organic solar cells and device efficiencies exceeding 3% have been reported [5] for a blend of poly[2-methoxy-5-3(3′,7′-dimethyloctyloxy)-1-4-phenylene vinylene], (MDMO-PPV), with 1-(3-methoxycarbonyl)-propyl-1-phenyl-(6,6)C_{61}, (PCBM). Very recently device efficiencies of over 5% have been claimed for a proprietary red absorbing polymer blended with PCBM [6]. Films of MDMO-PPV blended with PCBM have been extensively studied [7–10] and the function of such films is based on electron transfer from photogenerated excited states of the conjugated polymer to fullerene acceptors. Studies of the charge separation reaction show that electron transfer to the fullerene can occur in less than 100 fs [11] and that the quantum yield of photoinduced charge generation is close to 100% [2]. Efficient charge transport to the electrodes can only be achieved if charge recombination is sufficiently slow compared to charge separation because recombination is in competition with charge transport across the film to the device electrodes. It was thought [8] that the intimate blending of the two components may also facilitate interfacial charge recombination and that this would limit the efficiency of photovoltaic devices. However, recent studies on the recombination dynamics in thin films of MDMO-PPV:PCBM conclude that charge recombination is sufficiently slow not to limit photocurrent collection under solar intensities at short circuit [7]. Indeed, the high charge collection efficiency results in external quantum efficiencies of over 50% [12].

Understanding the mechanism of charge transport in single polymer materials and blends is therefore critical to the development of improved organic solar cells and other molecular electronic devices. Transport in organic electronic materials is traditionally studied by time resolved or steady state mobility measurements. The results are usually evaluated within a framework such as the Gaussian Disorder Model, (GDM), and its variants [13–15] where the field and temperature dependence of the charge carrier mobility are used to quantify

*Author to whom all correspondence should be addressed.

the degree of energetic and configurational disorder in the charge transport matrix. Although useful for comparative studies [10], these models are unhelpful for identifying the microscopic transport mechanism or for relating the charge transport properties to the chemical or physical structure of the materials. Moreover, they have as yet been applied only to single component systems and do not allow for the impact of geometry on transport in two-component blends.

We have developed Monte Carlo models of polaron transport in organic films which may be single component or binary systems. The model is based on a site-to-site hopping process within an energetically disordered medium. We have evaluated alternative microscopic models for the intermolecular transfer rate [16], and we find that a small-polaron hopping rate, based on non-adiabatic Marcus theory, is more appropriate than the commonly used 'symmetric' [15] and Miller-Abrahams [13] charge transfer expressions in the limit of ordered materials. In this work, we show that the transport behaviour detected by time of fight mobility measurements and transient absorption spectroscopy can be described quantitatively with a single transport model.

Transient absorption spectroscopy is a complementary probe of charge transport in polymer/molecule blends, where the population of polaronic species is monitored optically following photoexcitation [8, 9]. Unlike time of flight mobility studies, transient absorption probes transport in the low-field diffusion-limited regime, and in certain conditions the dynamics are dominated by polaron diffusion in a single component [7] and can be correlated with the experimentally observed mobility [10].

Studies of charge recombination in MDMO-PPV:PCBM blends using transient optical spectroscopy show kinetics with a slow phase whose amplitude saturates with increasing laser intensity. The slow phase decays as a power law with time and is thermally activated [8, 9]. This behaviour cannot be explained with simple models of diffusion limited or Coulomb-interaction driven recombination [7]. It is argued that the decay in the ms to μs time scale corresponds to the detrapping of localised hole polarons trapped below the mobility edge of the inhomogeneously broadened density of states for the material. Results in MDMO-PPV:PCBM blends are qualitatively compatible with a Monte Carlo model where charge recombination is limited by the trap-limited diffusion of positive polarons towards PCBM anions [7]. Polaron transport is mediated by thermally activated hopping between polymer sites with a density of states containing a small fraction of localised trap states with an exponential distribution of energies below the mean transport level.

2. Monte Carlo model

The time of flight Monte Carlo model is required to simulate the photoinduced displacement current density as a function of time after excitation by a laser pulse. The transport landscape for the carriers is modelled as a lattice of discrete sites with energies drawn from a density of states function $g(E)$. For hole measurements each site represents, approximately, one hole transporting unit and the lattice constant of 1 nm was chosen to correspond approximately to the mean inter-monomer distance. The different energies represent both energetic disorder due to conformational variation and deep traps due to chemical defects. The lattice sites are randomly assigned as donor or acceptor according to the volume fractions of the two components in the blend under study.

Carriers are generated according to the sample thickness, absorption coefficient and laser excitation density. The sequence of carrier motions is then determined by assigning each carrier a waiting time and destination according to the transport mechanism and sorting them into a queue. At each step in the iteration, the carrier with the shortest waiting time, t_1, moves to its destination, the simulation time is advanced by t_1 and the waiting time of all remaining carriers is reduced by t_1. The external field is applied in the z direction and periodic boundary conditions are applied in the x and y directions. If the carrier reaches the $z = L$ boundary it is removed from the queue. If not, it is assigned a new waiting time and destination and is re-entered into the queue. If the carrier moves in the z direction the current density is updated. The procedure is repeated for the carrier now at the top of the queue. The device of the queue enables several carriers to be handled at once. Trap filling effects are included through a rule preventing multiple occupancy of sites, thus ensuring consistency with Fermi-Dirac statistics.

Throughout the simulations the field is recalculated according to Poisson's equation and Gauss' law assuming a relative dielectric constant of 3. Thus the field is dependent on the carrier density across the film which itself varies with time throughout the simulations. At experimental laser intensities the effect of photoinjected charge on the field distribution was negligible. The current density, electric field, density of occupied site energies and carrier distribution are monitored throughout the simulations and averaged over the total number of simulations performed for a given set of conditions.

The relative transfer rates, ν_{ij}, from site i to nearest neighbour site j of the same component are given by the small polaron hopping rate [17] based on non-adiabatic Marcus theory:

$$\nu_{ij} = \nu_0 \exp\left[-\frac{(-\Delta - \lambda)^2}{4kT\lambda}\right] \tag{1}$$

where k is Boltzmann's constant, T is the thermodynamic temperature, ν_0 is a constant with dimensions of frequency and λ is the reorganisation energy. The parameter Δ is given by

$$\Delta = E_j - E_i - q\mathbf{a} \cdot \mathbf{F} \tag{2}$$

where E_{ij} are the occupied site energies of sites i and j, q is the charge of the carrier, $\mathbf{F}$ is the field vector and $\mathbf{a}$ is the lattice vector appropriate for the direction of the hop. This transport model obeys microscopic detailed balance such that for isoenergetic site energies the ratio

of forward and backward transfer rates between any two neighbouring sites is

$$\frac{\nu_{z+}}{\nu_{z-}} = \exp\left(\frac{q\mathbf{a}\cdot\mathbf{F}}{kT}\right) \tag{3}$$

The results of this model may thus be directly compared with simulations using other models in the literature [13–15]. Before the relevant wait time for a carrier on a site is calculated the destination site must be determined. The method employed here is essentially the same as that used in earlier Monte Carlo simulations of carrier mobilities [13], except that here hops to sites in the second component of the blend are forbidden. The probability of hopping to a given available nearest neighbour k is:

$$P_{ik} = \frac{\nu_{ik}}{\sum_j \nu_{ij}} \tag{4}$$

where the sum in the denominator is over the available nearest neighbours of the same component. Each site is given a length in random number space according to P_{ik} and a random number from a uniform distribution is chosen which thus specifies the destination site. The wait time τ for a carrier on a site is determined by

$$\tau = \frac{6(-\ln X)}{\sum_j \nu_{\mathrm{ij}}} \tag{5}$$

where X is a random number between 0 and 1.

Before addressing the experimental data, the reasons for the choice of density of states utilized in this work are first outlined. The transient optical data for freshly prepared films of MDMO-PPV: PCBM blends follow a power law of exponent ~0.4 over 4 orders of magnitude in time [8, 9]. Assuming that the change in absorption is proportional to the polaron density, p, this implies:

$$p \propto t^{-\alpha} \tag{6}$$

where α–0.4. Such power law kinetics are known to follow for a process that is limited by thermal activation from an exponential density of trap states of the form:

$$g_{\mathrm{t}}(E) = \frac{N_{\mathrm{t}}}{kT_0}\exp\left(\frac{E-E_0}{kT_0}\right) \tag{7}$$

where N_{t} is the total density of localised states and α is given by

$$\alpha = \frac{T}{T_0} \tag{8}$$

The best agreement between the data of Refs. [8, 9] and the Monte Carlo model [7] was achieved using a bimodal density of states containing a fraction $(1-\phi)$ of 'delocalised' states with energy close to the HOMO level, E_0, and a fraction ϕ of 'localised' trap states with energies drawn from the exponential distribution $g_{\mathrm{t}}(E)$ above. The delocalised fraction may be considered as lying above a mobility edge [7] and the energies of these states were taken from the ideal Gaussian distribution of states $g_{\mathrm{d}}(E)$ expected for very pure materials [13] which is given by

$$g_{\mathrm{d}}(E) = \frac{N_{\mathrm{d}}}{\sqrt{2\pi\sigma}}\exp\left[-\frac{(E-E_0)^2}{2\sigma^2}\right] \tag{9}$$

where σ is the half width of the distribution and N_{d} is the total density of delocalised states. In Ref. [7] a trap fraction of $\phi = 0.001$ and $\sigma/kT \sim 1$ was found to give good agreement with the experimental data. A very broad Gaussian density of states could produce an approximately power law dependence of $\alpha \sim 0.4$ but only over 2–3 orders of magnitude in time [7].

In this work we utilize the same density of states as used in [7] and show that for comparable trap fractions the resulting time of flight hole transients show very good agreement with experiment. More importantly, we also show that the field dependence of the mobility extracted from the transit times is also in close agreement with experiment.

The following physical assumptions are implicit in the model: (i) the quantum efficiency of exciton dissociation is unity, (ii) carrier transport occurs only by nearest neighbour hops and is forbidden on the second component in a binary blend, (iii) that recombination is negligible and, (iv) the geometry of the blend is a random distribution of donor and acceptor sites. Point (i) follows from experiment [2]. Point (iii) may be justified because the applied field accelerates carriers in opposite directions and, since they are generated mainly near the illuminated surface of the film, there is only a small distance over which they may interact resulting in recombination. Assumption (iv) holds for low concentrations of PCBM but AFM height and phase images [18] show that at weight fractions greater than 50% PCBM tends to phase segregate forming a globular structure within the blend.

3. Experimental details

This work focuses on pristine MDMO-PPV and a low concentration MDMO-PPV: PCBM blend with a composition of 3:1 by weight. Films were spin cast in chlorobenzene onto indium tin oxide (ITO) substrates and an aluminium counter electrode was evaporated onto the back of the film. The films of the pristine polymer and 3:1 blend were 1.1 and 1.2 μm thick respectively.

Devices were illuminated through the ITO electrode using a frequency-tripled 355nm Nd:YAG laser with an incident power such that the charge generated is less than 10% of CV, where C is the capacitance of the film and V is the applied bias. The ITO electrode was held at ground potential and the carrier type under study was selected by the sign of the bias voltage applied to the counter electrode using an Oxford Instruments power supply. The transient current produced by the laser pulse in the presence of an external applied electric field was then recorded by a Tektronix oscilloscope across a variable resistor. All the measurements were taken in air at room temperature, and experimental

mobilities, μ, were calculated according to:

$$\mu = \frac{d^2}{t_{\mathrm{tr}} V} \tag{10}$$

where d is the thickness of the film and t_{tr} is the transit time. The photocurrent transients obtained for the pristine polymer and 3:1 blend were characteristic of 'dispersive' charge transport and do not feature a plateau region followed by a sigmoidal decay when plotted on a linear scale. For such dispersive transients the transit time is generally taken as the point of intersection of the linear asymptotes when plotted in a double logarithmic representation.

4. Results

Experimental and simulated results are compared in order to test whether the density of states suggested from detailed transient absorption measurements [8, 9] and modelling [7] can also be used to explain both the field dependence of the hole mobility and the shape of the current transients measured in the time of flight experiments.

For the simulations of the time of flight current transients in both the pristine polymer and the 3:1 blend, 98% of the sites had energies drawn from the Gaussian distribution (Equation 9) with $\sigma / kT = 1$. The remaining 2% of sites had energies drawn from the exponential distribution (Equation 7) with a characteristic temperature T_0 of 750 K corresponding to $\alpha = 0.4$.

The system was simulated using a lattice of $51 \times 51 \times 1000$ sites, where the longest direction corresponds to the z direction in which the field was applied. This corresponds to a simulation volume of 2.6×10^{-15} cm^3, and, the relatively low intensity laser pulse results in 196 photogeneration events in this volume which are distributed according to the absorption coefficient at the laser wavelength and the film thickness. This corresponds to a charge density of 7.5×10^{16} cm^{-3} per pulse.

The charge transfer rates were calculated using the small polaron hopping expression (Equation 1) with a reorganisation energy $\lambda = 0.5$ eV which is well within the range of plausible values (0.1 to 0.9 eV) [17, 19]. Since there is no experimental data the reorganisation energy was treated as an adjustable parameter in this work. The value of α used was fixed at 0.4 by experimental measurements in Refs. [8, 9]. The trap fraction $\phi = 0.02$ was chosen to give the best agreement between the simulated and experimental current transients. For fixed α and ϕ, the results were relatively insensitive to the value of λ. The reorganisation energy may have a stronger influence on the temperature dependence of the mobility and the value of 0.5 eV may need to be revised in the light of further studies. The value of the scaling factor ν_0 was chosen to give the best fit to the timescales of the experimental current transients measured for the pristine polymer film.

4.1. Pristine polymer

In Fig. 1 typical experimental and simulated current transients for the film of pristine MDMO-PPV are illustrated in a linear plot for the highest electric field investigated. The model results were averaged over 100 simulations. The shapes of the simulated transients show an almost exact correspondence with those observed experimentally. As seen in Fig. 1 the timescale of the decay in the simulations agrees almost exactly with the experiment.

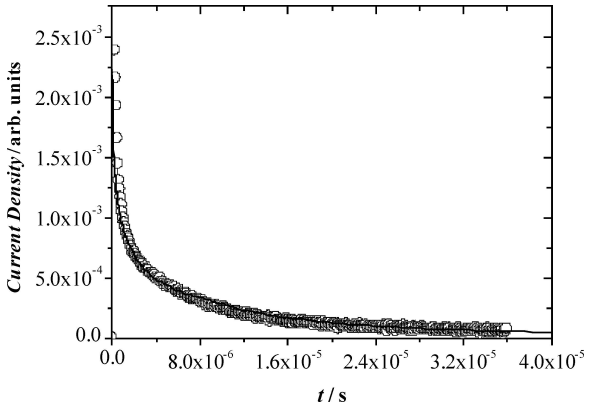

Figure 1 Simulated and experimental time of flight current transients in the pristine polymer at a high applied field of 6.36×10^5 V cm^{-1}. The open circles denote the experimental data and the solid line denotes the simulation results.

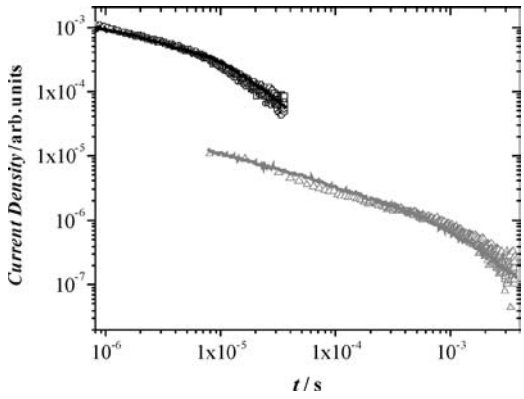

Figure 2 Simulated and experimental time of flight current transients in the pristine polymer at the highest and lowest applied fields plotted in a double logarithmic representation. The open black circles and open grey triangles denote the experimental data at the applied fields of 6.36×10^5 and 9.09×10^4 V cm^{-1} respectively, and the black and grey solid lines indicate the simulation results.

In Fig. 2 the same data is plotted in a double logarithmic representation together with the experimental and simulated results for the lowest electric field investigated. Fig. 2 shows that the transients become less dispersive at high field owing to field assisted activation of carriers out of deep traps.

4.2. 3:1 blend

The Monte Carlo model was unchanged for the simulations of the time of flight current transients in the 3:1 blend except that the fraction of hole transporting sites was reduced to 0.83 calculated assuming a MDMO-PPV density of $\sim$1 g cm^{-3} and a PCBM density of $\sim$1.6 g cm^{-3}. In Fig. 3 typical experimental and simulated current transients for the film of blended MDMO-PPV:PCBM (3:1 by weight) are illustrated in a linear plot for a low electric field. The model results were again averaged over 100 simulations. The shapes

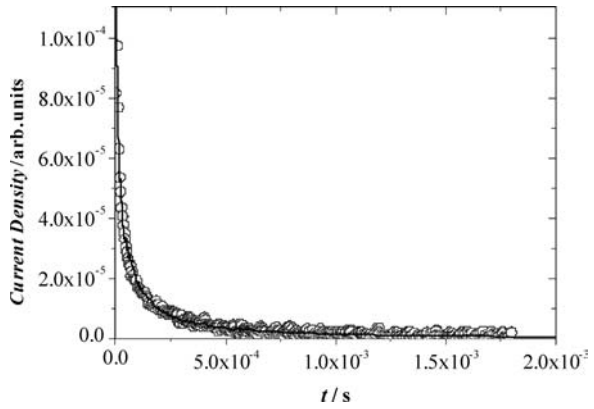

Figure 3 Simulated and experimental time of flight current transients in the 3:1 blend at a low applied field of 2.73×10^5 V cm^{-1}. The open circles denote the experimental data and the solid line denotes the simulation results.

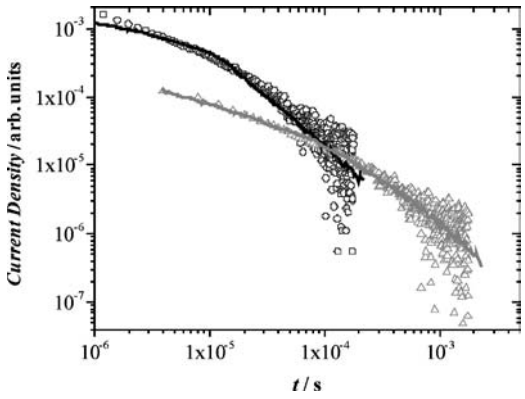

Figure 4 Simulated and experimental time of flight current transients in the 3:1 blend at high and low applied fields plotted in a double logarithmic representation. The open black circles and open grey triangles denote the experimental data at the applied fields of 5.45×10^5 and 2.73×10^5 V cm^{-1} respectively, and the black and grey solid lines indicate the simulation results.

of the experimental transients are very similar to those observed in the pristine polymer. Again, an almost exact correspondence is seen in Fig. 3 between the results of the simulations and experiment. This is also seen in Fig. 4 where the same data is plotted in a double logarithmic representation together with the transient for a high applied field.

4.3. Field and composition dependence of the mobility

Exactly as for the experimental data, the transit times for the results of the model were taken as the point of intersection of the linear asymptotes when plotted in a double logarithmic representation. The field dependence of the mobility calculated from the transit times of the experimental and simulated current transients are compared in Figs 5 and 6. In the double logarithmic plot (Fig. 5) the field dependence from the simulations is seen to be in good agreement with the experiment for both the pristine polymer and the 3:1 blend. In this figure it can be seen that both the experimental and simulated mobilities show Poole-Frenkel like behaviour, characterised by a linear dependence of the logarithm of the mobility on the square root of the applied field.

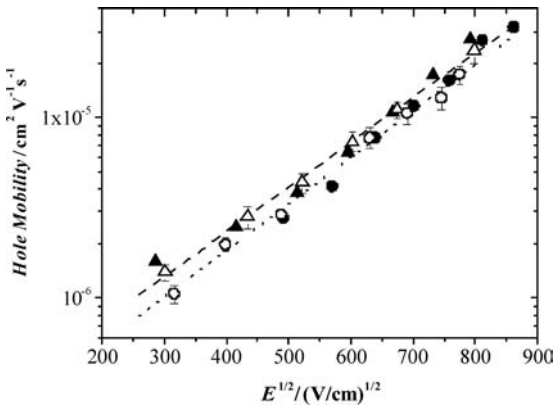

Figure 5 Logarithmic plot of the field dependence of the hole mobility extracted from the experimental and simulated current transients for both the pristine polymer and the 3:1 blend. The pristine polymer is denoted by triangles and the 3:1 blend is denoted by circles. Filled and open symbols are used for the experiments and simulations respectively. The lines are the best exponential fits to the simulation results where long dashes indicate the pristine polymer and short dashes indicate the 3:1 blend.

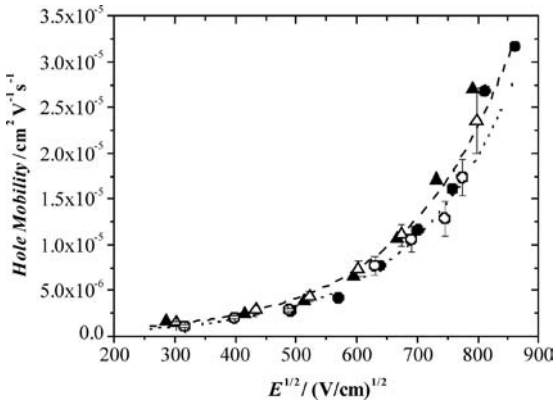

Figure 6 Linear plot of the field dependence of the hole mobility extracted from the experimental and simulated current transients for both the pristine polymer and the 3:1 blend. The pristine polymer is denoted by triangles and the 3:1 blend is denoted by circles. Filled and open symbols are used for the experiments and simulations respectively. The lines are the best exponential fits to the simulation results where long dashes indicate the pristine polymer and short dashes indicate the 3:1 blend.

It appears from Fig. 5 that the experimental data deviates slightly from the results of the model. The experimental data for the pristine polymer appear to show a slight curvature compared to the model results and the experimental data for the 3:1 blend appear to have a slightly stronger field dependence than the model. However, there is scatter in the experimental data and neither of these observations is conclusive.

In the linear plot (Fig. 6) it appears that there is very good agreement between the model and experiment at low fields but that at high fields the experiment deviates from both Poole-Frenkel behaviour and the model. The results of the modelling show Poole-Frenkel like behaviour over the full range of applied fields investigated without the need to invoke configurational disorder.

The predicted reduction in the mobility of the 3:1 blend compared to the pristine polymer is also in good agreement with that determined experimentally. This result proves that at low PCBM concentration that the PCBM fraction is effectively a barrier to hole transport.

5. Discussion

The predicted reduction in the mobility shown by the simulations on addition of 17% by volume PCBM is what would be expected if the polymer structure were unaltered by the low fraction of PCBM, which acts merely as a barrier to hole transport. Such a model is not expected to be applicable at high PCBM fractions because a 2 order of magnitude increase [20] in the hole mobility of MDMO-PPV:PCBM blends is observed at PCBM weight fractions over 50%. The reasons for this behaviour are not yet known with any certainty and Monte Carlo simulations with the aim of rationalising this trend will be the subject of future work.

The model of hole transport presented here has also been employed as part of a study on the effects of photo-oxidation on the properties of MDMO-PPV:PCBM blends [21]. In this work the value of α describing the exponential distribution of localised states detected by transient absorption spectroscopy changed from 0.4 to 0.2 on oxidation indicating a deeper distribution of traps. Time of flight measurements were again successfully simulated with the model described here taking the characteristic temperature of the exponential distribution of localised states directly from the transient optical measurements. However, in this case a lower fraction ϕ = 0.003 of localised states gave the best agreement between the experiments and simulations. In general the degree of disorder in dispersive conjugated polymer films such as MDMO-PPV is very sensitive to processing conditions. Therefore we do not find it unreasonable that the fraction ϕ of localised states required in order to obtain agreement between the model and experiment varies by an order of magnitude between studies.

6. Conclusions

We show that for pristine MDMO-PPV and a 3:1 by weight blend of MDMO-PPV, that the transport behaviour detected by time of flight and transient absorption spectroscopy can be described quantitatively with a single transport model. We find that Monte Carlo simulations of time of flight current transients utilising the density of states suggested from detailed measurements and modelling of transient absorption can also be used to explain the field dependence of the hole mobility and the shape of the current transients measured in the time of flight experiments.

We further show that for the low PCBM fraction blend that the reduction in hole mobility is consistent with PCBM acting only as a barrier to hole transport although this is probably not the case at higher PCBM fractions.

Acknowledgements

The authors would like to thank BP Solar and the EPSRC for financial support.

References

1. N. S. SARICIFTCI, D. BRAUN, C. ZHANG, V. I. SRDANOV, A. J. HEEGER, G. STUCKY and F. WUDL, *Appl. Phys. Lett.* **62** (1993) 582.
2. C. J. BRABEC, N. S. SARICIFTCI and J. C. HUMMELEN, *Adv. Funct. Mater.* **11** (2001) 15.
3. G. YU, J. GAO, J. C. HUMMELEN, F. WUDL and A. J. HEEGER, *Science* **270** (1995) 1789.
4. G. YU and A. J. HEEGER, *J. Appl. Phys.* **78** (1995) 4510.
5. C. J. BRABEC, S. E. SHAHEEN, C. WINDER, N. S. SARICIFTCI and P. DENK, *Appl. Phys. Lett.* **80** (2002) 1288.
6. SEIMENS AG, Press release, 07/01/04.
7. J. NELSON, *Phys. Rev. B* **67** (2003) 155209.
8. I. MONTANARI, A. F. NOGUIRA, J. NELSON, J. R. DURRANT, C. WINDER, M. A. LOI, N. S. SARICIFTCI and C. BRABEC, *Appl. Phys. Lett.* **81** (2002) 3001.
9. A. F. NOGUIRA, I. MONTANARI, J. NELSON, J. R. DURRANT, C. WINDER, N. S. SARICIFTCI and C. BRABEC, *J. Phys. Chem. B* **107** (2003) 1567.
10. S. A. CHOULIS, J. NELSON, Y. KIM, T. KREOUZIS, J. R. DURRANT, D. D. C. BRADLEY and J. C. HUMMELEN, *Appl. Phys. Lett.* **83** (2003) 3812.
11. C. J. BRABEC, G. ZERZA, G. CERULLO, S. DE SILVESTRI, S. LUZZATI, J. C. HUMMELEN and N. S. SARICIFTCI, *Chem. Phys. Lett.* **340** (2001) 232.
12. S. E. SHAHEEN, C. J. BRABEC, N. S. SARICIFTCI, F. PADINGER, T. FROMHERZ and J. C. HUMMELEN, *Appl. Phys. Lett.* **78**(6) (2001) 841.
13. H. BASSLER, *Phys. Status Solidi B* **175** (1993) 15.
14. S. V. NOVIKOV, D. H. DUNLAP, V. M. KENKRE, P. E. PARRIS and A. V. VANNIKOV, *Phys. Rev. Lett.* **81** (1998) 4472.
15. Z. G. YU, D. L. SMITH, A. SAXENA, R. L. MARTIN and A. R. BISHOP, *Phys. Rev. Lett.* **84** (2000) 721.
16. A. J. CHATTEN *et al.*, in preparation.
17. J. STEPHAN, S. SCHRADER and L. BREHMER, *Syn. Metals* **111/112** (2000) 353.
18. J. K. J. VAN DUREN, X. YANG, J. LOOS, C. W. T. BULLE-LIEUWMA, A. B. SIEVAL, J. C. HUMMELEN and R. A. J. JANSSEN, *Adv. Funct. Mater.* (2004) in press.
19. N. E. GRUHN, D. A. DA SILVA FILHO, T. G. BILL, M. MALAGOLI, V. COROPCEANU, A. KHAN and J.-L. BREDAS, *J. Am. Chem. Soc.* **124** (2002) 7918.
20. S. M. TULADHAR *et al.*, in preparation.
21. R. PACIOS *et al.*, in preparation.